Block Copolymer Self-Assembly in Selective Solvents: Theory of Solubilization in Spherical Micelles

R. Nagarajan* and K. Ganesh

Department of Chemical Engineering, The Pennsylvania State University, 161, Fenske Laboratory, University Park, Pennsylvania 16802. *Received December 13, 1988; Revised Manuscript Received April 1, 1989*

ABSTRACT: A theory of solubilization of low molecular weight compounds J in micelles of AB diblock copolymer formed in a selective solvent S is developed in this paper. The treatment assumes a spherical structure for the micelles. In these spherical micelles, it is visualized that the solvent S and the solvent-compatible B block of the copolymer are entirely excluded from the core region, whereas almost all of the solubilizate molecules J are located within. The free energy of solubilization has been modeled taking into account the variations in the states of deformation and in the states of dilution of the polymer blocks, the formation of the micellar interface, and the localization of the copolymer, all accompanying the solubilization process. On the basis of this free energy model, the theory permits the prediction of the critical micelle concentration, the size and composition distribution of the micelles containing solubilizates, the aggregation number of the micelles, the maximum extent of solubilization, and the core radius and the shell thickness of the micelles. Illustrative calculations show that, in general, the micelles are practically monodispersed both in their size and in the extent of solubilization. The solubilization behavior of the micelles and their geometrical characteristics are found to be significantly influenced by the interactions between the solubilizate J and the solvent-incompatible A block of the copolymer as well as by the solubilizate J–solvent S interfacial tension. The micellar structural parameters are affected also by the interactions between the solvent S and the solvent-compatible B block of the copolymer though to a somewhat lower degree when compared to the corresponding solubilizate-free systems. Generalized scaling relations have been developed that explicitly relate the micelle core radius, the shell thickness, and the volume fraction of the solubilizate within the micelle core to the molecular features of the copolymer, the solvent, and the solubilizate. The predictions of the present theory have been compared against our earlier experimental data on the solubilization of hydrocarbons in aqueous solutions of diblock copolymers.

Introduction

Copolymers are produced by the simultaneous polymerization of more than one type of monomer. The product resulting from such synthesis is known as a block copolymer if the monomers occur as blocks of various lengths in the product copolymer. For example, a diblock copolymer of type $[A_kB_m]$ consists of a block of k repeating units of kind A covalently bonded to a block of m repeating units of kind B. The two different types of blocks within the copolymer are usually incompatible with one another. A consequence of this mutual incompatibility among the two blocks is the interesting phenomenon of self-assembly in pure block copolymers as well as in solutions of block copolymers.[1-3] For example, when a AB diblock copolymer is present in solvent S, which is selective for B, the copolymer spontaneously organizes itself in such a way that the resulting microstructure consists of a core region made up of the A blocks and a surrounding shell region consisting of the B blocks and the solvent S. Such a microstructure generated by block copolymers in solutions resembles, in all essential aspects, the well-known micellar aggregates formed from a variety of low molecular weight surfactants.

A distinguishing feature of micellar systems is their ability to enhance the solubility of compounds that otherwise display very low solubility in the pure solvent. This occurs because the core of the micelle, which is incompatible with the solvent, provides a suitable microenvironment for the solubilizate, which is also incompatible with the solvent. Consequently, the extent of dissolution of the solubilizate in micellar solutions is dramatically enhanced when compared to that in the pure solvents. This phenomenon, known as solubilization or microemulsification, constitutes the basis on which a vast number of practical applications of surfactants are realized. The phenomenon of solubilization has been studied extensively in aqueous and nonaqueous solutions of low molecular weight conventional surfactants. In contrast, there have been virtually no studies of the solubilization tendencies of low molecular weight solubilizates in block copolymer micelles. In an earlier paper,[4] we presented some preliminary experimental results on the solubilization of hydrocarbons in micelles formed of two water-soluble block copolymers, namely, poly(ethylene oxide)–poly(propylene oxide) (PEO–PPO) and poly(vinyl pyrrolidone)–poly(styrene) (PVP–PS). In these two cases, micelles form in water with poly(propylene oxide) and polystyrene, respectively, constituting the micellar core. The maximum amount of solubilization of aromatic and aliphatic hydrocarbons in these micelles was measured by contacting the aqueous block copolymer micellar solutions against pure hydrocarbon phases as well as binary mixtures of hydrocarbons. The measurements suggested that the extent of solubilization is dependent on the nature of interactions between the solubilizate and the block that constitutes the core of the micelle. More interestingly, the measurements revealed unusual selectivity in the solubilization behavior when mixtures of hydrocarbons were solubilized. For example, aromatic molecules were found to be solubilized preferentially compared to aliphatic hydrocarbons.

No theoretical treatment of solubilization of low molecular weight compounds in block copolymer micelles is currently available. Evidently, a theory of solubilization can be used to explain the observed solubilization capacities for hydrocarbons in aqueous solutions and the selectivity in this solubilization behavior. Further, block copolymers hold unusual potential compared to conventional low molecular weight surfactants because of their ability to micellize in a variety of solvents. Consequently, one can visualize microemulsions involving two nonaqueous solvents formulated using block copolymers as the interfacial agents. Such systems cannot usually be obtained through the use of conventional low molecular

* To whom all correspondence should be addressed.

0024-9297/89/2222-4312$01.50/0

weight surfactants. To design block copolymer systems exhibiting such solubilization and microemulsification behavior, a fundamental theory of solubilization will be useful.

A theory of solubilization could be developed in principle by following the theoretical approaches to the formation of micelles pioneered by de Gennes,[5] Leibler et al.,[6] and Noolandi and co-workers.[7,8] In these treatments, the solvent-compatible B block is considered to have little or no influence on the characteristics of the micelles formed. An alternate treatment of block copolymer micelles in selective solvents was formulated by us earlier,[9] utilizing an approach that has successfully been applied to conventional surfactant micelles. The novel outcome of this theory, in contrast to the treatment of micellization developed by de Gennes,[5] Leibler et al.,[6] and Noolandi and Hong,[7] is its prediction that the micellization behavior is strongly influenced by the interactions between the solvent S and the solvent-compatible B block of the copolymer. This characteristic behavior is more prominent in those systems where the compatibility between the B block and the solvent S is very good. In the present paper, we extend our treatment of micellization to develop a theory of solubilization in block copolymer micelles present in selective solvents.

The present treatment considers the block copolymer–solvent–solubilizate system to be a multicomponent solution consisting of solvent molecules, singly dispersed copolymer molecules, singly dispersed solubilizate molecules and micelles of all sizes containing various possible amounts of the solubilizates. By minimizing the free energy of this multicomponent solution, an expression for the equilibrium size and composition distribution of micelles containing the solubilizates is obtained.[10] To calculate explicitly the structural properties of the micelles, one requires an expression for the difference in the reference state free energy between a micelle and the singly dispersed block copolymer and solubilizate molecules. Such an expression is formulated here. Illustrative calculations of the solubilization behavior have been carried out as a function of the copolymer and solvent characteristics for different types of copolymer–solvent systems and a variety of solubilizates. Utilizing the results of these numerical calculations, generalized scaling relations have been developed between the radius of the micellar core R, the thickness of the micellar shell D, the aggregation number of the micelle g, and the volume fraction of the solubilizate inside the micellar core region η, on the one hand, and the molecular properties of the copolymer, the solvent, and the solubilizate, on the other. These scaling relations facilitate direct comparison of the experimental data against the predictions of the present theory. In this paper, only spherical micelles and low molecular weight solubilizates are considered. In a latter paper, models for solubilization in rodlike and lamellar micelles and for solubilization of homopolymeric solutes will be presented.

Thermodynamics of Solubilization

We consider a solution consisting of solvent molecules, singly dispersed copolymer and solubilizate molecules, and micellar aggregates. The micelles are made up of g block copolymer and j solubilizate molecules where g and j are allowed to assume all possible values. Each of the above species, including micelles of different sizes and compositions, is treated as a distinct chemical component. The standard state of the solvent is defined to be that of pure solvent, whereas the standard states of all the other components are taken to be those corresponding to infinitely dilute solution conditions. We denote by μ°_s, μ°_1, μ°_{1J}, and μ°_{gj}, the standard chemical potentials of the solvent, the singly dispersed copolymer, the singly dispersed solubilizate, and micelles of aggregation number g containing j solubilizate molecules, respectively. The distribution of micelle size and composition at equilibrium can be obtained by minimizing the total free energy of the system.[10] Denoting the mole fraction of species i by X_i, the micelle size and composition distribution equation can be written in the form

$$X_{gj} = X_1^g X_{1J}^j \exp\left[-\left(\frac{\mu^\circ_{gj} - g\mu^\circ_1 - j\mu^\circ_{1J}}{kT}\right)\right] \quad (1)$$

In writing eq 1, we assume that intermicelle interactions are either not present or that they do not affect the size distribution expression. Also the system entropy of the multicomponent solution is written as for an ideal solution. Alternately, if the system entropy is written in terms of the Flory–Huggins model, the following expression for the aggregate size and composition distribution is obtained:

$$\phi_{gj} = \phi_1^g \phi_{1J}^j \exp(g + j - 1) \exp\left[-\left(\frac{\mu^\circ_{gj} - g\mu^\circ_1 - j\mu^\circ_{1J}}{kT}\right)\right] \quad (2)$$

In eq 2, ϕ_i denotes the volume fraction of the species i in the total solution. In general, the expression for the aggregate size and composition distribution depends on the assumptions pertaining to the system entropy as well as the nature of interaggregate interactions. In dilute solutions such as those of interest here, the intermicellar interactions are not important. Therefore, one may neglect the free energy contributions associated with such interactions. The consequences of using a few plausible models of system entropy in the theory of micellization have been analyzed in detail in an earlier paper.[11] It was found that the choice of a model for the system entropy affects only the magnitude of the critical micelle concentration (cmc) and has no influence on the micellar size parameters, for nonionic systems such as those considered in this paper. Also, the value for the cmc predicted on the basis of one of the entropy models can be simply related to those predicted on the basis of alternate entropy models.[11] Consequently, the principal conclusions of this paper are unaffected by the choice of the entropy models and the corresponding equations for the aggregate size and composition distribution.

From the size distribution equation, various size-dependent properties of the solution can be computed. The number-, weight-, and z-average aggregation numbers of the micelles are defined respectively by the relations

$$g_n = \sum gX_{gj}/\sum X_{gj}, \quad g_w = \sum g^2X_{gj}/\sum gX_{gj}, \quad g_z = \sum g^3X_{gj}/\sum g^2X_{gj} \quad (3)$$

The average molar ratio of the solubilizate to the block copolymer molecules in the micelle is calculated from

$$(j/g)_{av} = \sum jX_{gj}/\sum gX_{gj} \quad (4)$$

In the above two equations, the summation refers to that over the aggregation number g as well as the number of solubilizate molecules j contained within a micelle. If one wants to calculate the maximum amount of solubilization of a compound that is possible inside the micelle, then the concentration of the singly dispersed solubilizate X_{1J} or ϕ_{1J} is assigned a value equal to the saturation concentration of the solubilizate in the pure solvent. Corresponding to this condition, the micelle size and composition distribu-

tion equation can be simplified to

$$X_{gj} = X_1^g \exp\left[-\left(\frac{\mu^\circ_{gj} - g\mu^\circ_1 - j\mu^*_{1J}}{kT}\right)\right] \quad (5)$$

if the Ideal Solution model for the system entropy is used and to

$$\phi_{gj} = \phi_1^g \exp(g-1) \exp\left[-\left(\frac{\mu^\circ_{gj} - g\mu^\circ_1 - j\mu^*_{1J}}{kT}\right)\right] \quad (6)$$

if the Flory–Huggins model for the system entropy is used. The standard state of the solubilizate μ^*_{1J} appearing in the above equations refers to a pure solubilizate phase.[10]

The micelle containing the solubilizates can also be represented as a pseudophase in equilibrium with the singly dispersed solubilizate and copolymer molecules in solution. This is a convenient simplification generally used in the theory of micellization. Obviously, for narrowly dispersed systems, this representation provides results practically equivalent to those obtained from the detailed size distribution calculations. The equilibrium characteristics of the micelle in the pseudophase approximation are obtainable from the condition

$$\frac{\partial}{\partial g}\left(\frac{\mu^\circ_{gj}/g - \mu^\circ_1 - (j/g)\mu^*_{1J}}{kT}\right) = 0$$

$$\frac{\partial}{\partial j}\left(\frac{\mu^\circ_{gj}/g - \mu^\circ_1 - (j/g)\mu^*_{1J}}{kT}\right) = 0 \quad (7)$$

The critical micelle concentration (cmc) in the pseudophase approximation is calculated from eq 5 to be

$$(X_1)_{cmc} = \exp\left(\frac{\mu^\circ_{gj}/g - \mu^\circ_1 - (j/g)\mu^*_{1J}}{kT}\right) \quad (8)$$

Alternately, if eq 6 for the micelle size distribution is used, then the cmc can be calculated from

$$(\phi_1)_{cmc} = \frac{1}{e}\exp\left(\frac{\mu^\circ_{gj}/g - \mu^\circ_1 - (j/g)\mu^*_{1J}}{kT}\right) \quad (9)$$

The quantity $(\mu^\circ_{gj}/g - \mu^\circ_1 - (j/g)\mu^*_{1J})$ appearing in eq 5 and in various subsequent expressions represents the change in the reference state free energy when a singly dispersed block copolymer molecule from the solution and j/g solubilizate molecules from their pure phase are transferred into an isolated micelle in the solution. The magnitude of this free energy difference controls the cmc as shown by eq 8 and 9. In contrast, the equilibrium structural features of the micelle are determined by how this free energy difference depends on the variables g and j, as is evident from eq 7. At this stage, in order to formulate an expression for this free energy difference, the geometrical features of the micelle should be specified.

Geometrical Properties of the Micelle. In the present theory, the micelles are assumed to be spherical. Two closely related spherical structures can be visualized (Figure 1), in analogy with the structural models for solubilization and microemulsions in systems involving low molecular weight surfactants.[10] Figure 1a is typically used to represent solubilization while Figure 1b is used to denote droplet microemulsions. In the structure shown in Figure 1a, the micellar core is made up of the solvent-incompatible A blocks and the solubilizate J. The solvent-compatible B blocks and solvent S are present in the spherical shell

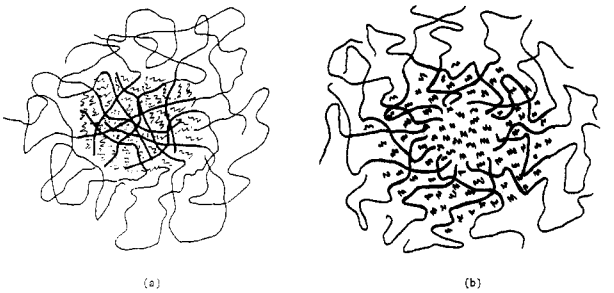

Figure 1. Schematic representation of a spherical micelle containing the solubilizate. The darker lines denote solvent-incompatible block A, while the lighter lines refer to solvent-compatible block B. The solvent molecules S are not shown in the figure. (a) In this mode of solubilization, the solubilizate molecules J are shown to be present within the core region only as a solution with the A blocks. (b) In this mode of solubilization, a region of pure solubilizate J constitutes the inner core. This inner core region is surrounded by a shell where the solubilizate J is present as a solution with the A blocks.

region of the micelle. The variables R and D denote the core radius and the shell thickness, respectively, of a micelle having an aggregation number g and containing j number of solubilizate molecules. The volume fraction of the solubilizate molecules within the core region of the micelle is denoted by η. v_A and v_B denote the molecular volumes of blocks A and B of the copolymer, while v_S and v_J denote the molecular volumes of the solvent and the solubilizate, respectively. $m_A = v_A/v_S$, $m_B = v_B/v_S$, and $m_J = v_J/v_S$ are the ratios of the molecular volumes of block A, block B, and the solubilizate J to that of the solvent S, respectively. The geometry of the micelle along with the assumption of incompressibility gives rise to the three equations that completely describe the structure of the spherical micelle:

$$V_C = gv_A + jv_J = \frac{4\pi R^3}{3} \quad (10)$$

$$V_{SH} = \frac{4\pi}{3}[(R+D)^3 - R^3] \quad (11)$$

$$\eta = \frac{jv_J}{gv_A + jv_J} \quad (12)$$

V_C and V_{SH} denote the volumes of the core and the shell regions of the micelle, respectively. Thus, a complete description of the micelle requires the specification of the three independent variables, namely, g, j, and D or, alternately, R, η, and D.

The structure shown in Figure 1b is analogous to that used for droplet microemulsions. Here, a region of pure solubilizate J is allowed to exist within the micellar core. This core is surrounded by an inner shell region consisting of the solvent-incompatible block A and the solubilizate J while the outer shell of the micelle contains the solvent-compatible block B and the solvent S. When compared to the model shown in Figure 1a, this alternate model differs in two important respects. The solubilizate J is present as a pure fluid in the core and as a solution in the inner shell; the solvent-incompatible block A stretches over only the inner shell region and does not extend to the center of the micelle. Obviously, in the absence of a pool of pure solubilizate J in the core, this alternate model reduces identically to that shown in Figure 1a. Free energy calculations of the kind described below when applied to this alternate model showed that the condition of minimum free energy always occurred corresponding to a zero size for the pure solubilizate pool. Thus, the thermodynamic equilibrium criterion always favored

the occurrence of the structure shown in Figure 1a rather than the alternate structure in Figure 1b. Consequently, the free energy expressions provided in this paper correspond to the model of micelle shown in Figure 1a.

Free Energy of Solubilization. An expression for the free energy of solubilization can be developed by considering all the physicochemical changes accompanying the transfer of the solubilizate molecules from their pure phase and the singly dispersed copolymer molecules from the solution to an isolated micelle also in the solution. This expression can be viewed as an extension of our earlier free energy model for micellization.[9] First, the transfer of the solubilizate and the singly dispersed AB diblock copolymer to the micellar core is associated with changes in the state of dilution and in the state of deformation of the A block. There is also the swelling of the A blocks inside the micellar core by the solubilizate J. Second, the B block of the singly dispersed copolymer is transferred to the solvent-penetrated shell region of the micelle. This transfer process also involves changes in the states of dilution and deformation of the B block. Third, the formation of the micelle localizes the copolymer such that the solvent-incompatible A block is confined to the core, while the solvent-compatible B block is confined to the shell. Finally, the formation of the micelle is accompanied by the generation of an interface between the micellar core made up of A blocks and the solubilizate J and the micelle shell consisting of the solvent S and the B blocks. Thus the free energy of solubilization is the sum of the above contributions. One may write

$$(\mu^\circ_{gj}/g - \mu^\circ_1 - (j/g)\mu^*_{1J}) = \Delta\mu^\circ_g = (\Delta\mu^\circ_g)_{A,dil} + (\Delta\mu^\circ_g)_{A,def} + (\Delta\mu^\circ_g)_{B,dil} + (\Delta\mu^\circ_g)_{B,def} + (\Delta\mu^\circ_g)_{loc} + (\Delta\mu^\circ_g)_{int} \quad (13)$$

Expressions for each of the free energy contributions denoted by $\Delta\mu^\circ_g$ in eq 13 are formulated below. One may consult for details ref 9, where the analogous expressions for the formation of micelles in the absence of solubilizates are developed. In obtaining the expressions for the change in the states of dilution and deformation of the A and the B blocks, we assume that the concentrations in the core and the shell regions are uniform. An alternate approach allowing for concentration inhomogeneities in the two regions will be discussed in a latter paper. Further, we consider the deformation of the chains to be characterized by uniform stretching along the length of the chain. Probably, a better description would involve nonuniform stretching of the chains, as it would be more compatible with the assumption of uniform concentrations in the core and the shell. Alternate equations based on nonuniform chain deformation are presented in the Appendix along with a discussion of how the main predictions of this paper will be correspondingly modified.

Change in State of Dilution of Block A. In the singly dispersed copolymer molecule, the A block is in a collapsed state, minimizing its interactions with the solvent. We consider the region consisting of the collapsed A block with some solvent entrapped to be a spherical globule, whose diameter $2R_{\infty A}$ is equal to the end-to-end distance of block A in the solvent. The volume of this spherical region is denoted by $v_{\infty A}$.

$$v_{\infty A} = \frac{4\pi R_{\infty A}^3}{3}, \qquad 2R_{\infty A} = \alpha_A m_A^{1/2} l \quad (14)$$

Here, l is the characteristic segment length, which is calculated from the volume of the solvent molecule as $l = v_S^{1/3}$. The chain expansion parameter α_A describes the swelling of the polymer block A by the solvent S and it can be estimated by following the method suggested by de Gennes.[12] On that basis one obtains[9]

$$\alpha_A = (6/\pi)^{1/3} m_A^{-1/6} \phi_p^{-1/3} \quad (15)$$

In the above equation, ϕ_p is the volume fraction of A within the monomolecular globule. It is calculated[12] from the condition of osmotic equilibrium between the monomolecular globule treated as a distinct phase and the solvent surrounding it. ϕ_p is obtained[9] as the solution of

$$\ln(1 - \phi_p) + \phi_p + \chi_{AS}\phi_p^2 = 0 \quad (16)$$

χ_{AS} in eq 16 refers to the Flory–Huggins interaction parameter between the pure A polymer and the solvent S. The state of the A block within the singly dispersed AB copolymer is thus specified. The state of the A block within the micelle is defined by the A block being confined to the core region where it is swollen by the solubilizate J. As mentioned earlier, we consider this region to be uniform in concentration, thus allowing a mean-field description of the free energy of this region.

One can thus estimate how the difference in the state of dilution of block A contributes to the free energy of solubilization from the following relation

$$\frac{(\Delta\mu^\circ_g)_{A,dil}}{kT} = \left[\frac{v_A}{v_J}\frac{\eta}{1-\eta}\ln\eta + \chi_{AJ}\eta\frac{v_A}{v_J}\right] - \left[\left(\frac{v_{\infty A} - v_A}{v_S}\right)\ln\left(\frac{v_{\infty A} - v_A}{v_{\infty A}}\right) + \chi_{AS}\left(\frac{v_{\infty A} - v_A}{v_S}\right)\left(\frac{v_A}{v_{\infty A}}\right) + \left(\frac{\sigma_{AS}}{kT}\right)4\pi R_{\infty A}^2\left(\frac{v_A}{v_{\infty A}}\right)\right] \quad (17)$$

In the above equation, the first two terms account for the entropic and enthalpic contributions arising from the mixing of pure A block and the pure solubilizate J within the micellar core. They are written in the form of the Flory expression for the swelling of a network[13] by a solvent. The third and the fourth terms account for the entropic and enthalpic changes associated with the removal of A block from its infintely dilute condition to a pure A state. These terms are written in the framework of the Flory expression[13] for an isolated polymer molecule. The last term accounts for the fact that the interface of the monomolecular globule disappears on micellization.[9] This term is written as the product of the surface area of the monomolecular globule and an effective interfacial tension, $\sigma_{AS}(v_A/v_{\infty A})$. Here σ_{AS} is the interfacial tension between pure A and solvent S. The additional factor $(v_A/v_{\infty A})$, which is the volume fraction of the polymer A in the monomolecular globule, takes into account the reduction in this interfacial tension caused by the presence of some solvent molecules inside the monomolecular globule.

Change in State of Deformation of Block A. The A block is stretched within the micelle over a length equal to the radius R of the micellar core. The free energy of this deformation compared to the unperturbed end-to-end distance of block A can be estimated by using the Flory model[13] for the deformation of a polymer chain along one direction, keeping the volume of the molecule constant. In the singly dispersed state of the copolymer, the conformation of the A block is characterized by the chain expansion parameter α_A, which is the ratio between the actual end-to-end distance and the unperturbed end-to-end distance of the polymer block A. The free energy of this deformation is written by using the Flory expression[13] derived for an isolated polymer molecule. On this basis, one obtains[9]

$$\frac{(\Delta\mu^\circ_g)_{A,def}}{kT} = \left[\frac{1}{2}\left(\frac{R^2}{m_A l^2} + 2\frac{m_A^{1/2} l}{R} - 3\right)\right] - \left[\frac{3}{2}(\alpha_A^2 - 1) - \ln \alpha_A^3\right] \quad (18)$$

In eq 18, the first term defines the A block deformation free energy in the micelle, while the second term defines the corresponding free energy in the singly dispersed copolymer. As mentioned earlier, in representing the free energy of deformation of the A block within the micelle, the above equation assumes that the chain is uniformly stretched along the length of the chain. An alternate model allowing for nonuniform chain deformation is discussed in the Appendix.

Change in State of Dilution of Block B. In the singly dispersed state of the copolymer, the polymer block B is swollen with the solvent. We consider this swollen B block to be a sphere, whose diameter $2R_{\infty B}$ is equal to the end-to-end distance of isolated block B in the solvent. The volume of this spherical region $v_{\infty B}$ is

$$v_{\infty B} = 4\pi R_{\infty B}^3/3, \qquad 2R_{\infty B} = \alpha_B m_B^{1/2} l \quad (19)$$

where the chain expansion parameter α_B is estimated by using the expression developed by Flory.[13] In the Flory expression for α_B, Stockmayer[14] has suggested decreasing the numerical coefficient by approximately a factor of 2 to ensure consistency with the results calculated from perturbation theories of excluded volume. Consequently, one can obtain[9] α_B as the solution of

$$\alpha_B^5 - \alpha_B^3 = 0.88(1/2 - \chi_{BS}) m_B^{1/2} \quad (20)$$

The state of the B block within the singly dispersed copolymer is thus specified. Within the micelle, the B blocks are present in the solvent-penetrated shell region of volume V_{SH}. We consider this shell region to be uniform in concentration.

Based on the definitions of the states of dilution of the B block in the micelle and in the singly dispersed state, one can write an expression for the corresponding contribution to the free energy of micellization.

$$\frac{(\Delta\mu^\circ_g)_{B,dil}}{kT} = \left[\left(\frac{V_{SH} - g v_B}{g v_S}\right)\ln\left(\frac{V_{SH} - g v_B}{V_{SH}}\right) + \chi_{BS}\left(\frac{V_{SH} - g v_B}{g v_S}\right)\left(\frac{g v_B}{V_{SH}}\right)\right] - \left[\left(\frac{v_{\infty B} - v_B}{v_S}\right)\ln\left(\frac{v_{\infty B} - v_B}{v_{\infty B}}\right) + \chi_{BS}\left(\frac{v_{\infty B} - v_B}{v_S}\right)\left(\frac{v_B}{v_{\infty B}}\right)\right] \quad (21)$$

The first two terms in eq 21 describe the entropic and enthalpic contributions to the free energy of swelling of the B block by the solvent in the shell region of the micelle, while the last two terms refer to the corresponding contributions in the singly dispersed copolymer molecule.

Change in State of Deformation of Block B. In the singly dispersed state, the B block has a chain conformation characterized by the chain expansion parameter α_B, which is the ratio between the actual end-to-end distance of the chain and the unperturbed end-to-end distance of the chain. Within the micelle, the B block is stretched over a length equal to the thickness D of the micellar shell. The difference between these deformation states provides a contribution to the free energy of micellization, which can be written analogous to that for A blocks. One obtains

$$\frac{(\Delta\mu^\circ_g)_{B,def}}{kT} = \left[\frac{1}{2}\left(\frac{D^2}{m_B l^2} + 2\frac{m_B^{1/2} l}{D} - 3\right)\right] - \left[\frac{3}{2}(\alpha_B^2 - 1) - \ln \alpha_B^3\right] \quad (22)$$

The first term in eq 22 represents the free energy of deformation of the B block in the micellar shell, while the second term denotes the corresponding free energy in the singly dispersed copolymer molecule. Both terms are written with respect to the unperturbed dimension of the B block. As in eq 18, here also the chain deformation free energy within the micelle is written assuming uniform chain stretching. An alternate expression based on nonuniform chain stretching is presented in the Appendix.

Localization of the Copolymer Molecule. As a result of micellization, the copolymer becomes localized in the sense that the joint linking blocks A and B in the copolymer is constrained to remain in the interfacial region rather than occupying all the positions available in the entire volume of the micelle. The entropic reduction associated with localization is modeled by the concept of configurational volume restriction. Thus, the localization free energy is calculated on the basis of the ratio between the volume available to the A–B joint in the interfacial shell of the micelle (surrounding the core and having a thickness l) and the total volume of the micelle:

$$\frac{(\Delta\mu^\circ_g)_{loc}}{kT} = -\ln\left(\frac{4\pi R^2 l}{\frac{4\pi}{3}(R + D)^3}\right) = -\ln\left(\frac{3R^2 l}{(R + D)^3}\right) \quad (23)$$

Free Energy of Formation of the Micellar Core–Solvent Interface. When a micelle forms, an interface is generated between a core region consisting of the A block and the solubilizate J and a shell region consisting of the solvent S and the B block. The free energy of formation of this interface can be estimated as the product of the surface area of the micellar core and an interfacial tension characteristic of this interface. The appropriate interfacial tension is that between a solution of block A in solubilizate J within the micelle core and a solution of block B in solvent S within the micellar shell. Since the shell region is often very dilute in block B, the interfacial tension can be approximated to be that between the solvent S and a solution of the A block with the solubilizate J within the core. Indeed, there is no conceptual difficulty in correcting for the presence of the B block in the shell region. For the purposes of this treatment, this refinement is viewed unnecessary and therefore will not be introduced here. Noting that the pure polymer A–solvent S interfacial tension is σ_{AS}, the free energy of generation of the micellar core–solvent interface is calculated from

$$\frac{(\Delta\mu^\circ_g)_{int}}{kT} = \left(\frac{\sigma_{AS}(1 - \eta) + \sigma_{SJ}\eta}{kT}\right)\left(\frac{4\pi R^2}{g}\right) \quad (24)$$

The interfacial tension σ_{SJ} refers to the macroscopic interfacial tension between the solvent S and the solubilizate J, while the interfacial tension σ_{AS} refers to a sharp interface between pure A polymer and a highly incompatible solvent S.

In writing eq 24, we have used the approximation that the interfacial tension of a polymer solution of block A in solubilizate J against another liquid S is the composition averaged interfacial tensions of pure polymer A and pure solubilizate J against the solvent S. The volume fraction is used as the composition variable. Such a linear de-

Table I
Molecular Properties of Solubilizate Systems

J	v_J, Å^3	χ_{AJ}	σ_{SJ}, dyn/cm	χ_{AS}	χ_{BS}
	A = PPO,	B = PEO,	S = Water		
benzene	148.4	0.0015	33.9	2.1	0.2
o-xylene	200.0	0.0180	36.1	2.1	0.2
ethylbenzene	204.0	0.0510	38.4	2.1	0.2
toluene	176.0	0.0280	36.1	2.1	0.2
cyclohexane	179.0	0.2180	50.2	2.1	0.2
n-hexane	218.5	0.8740	50.7	2.1	0.2
n-heptane	243.0	0.8940	51.2	2.1	0.2
n-octane	270.0	0.7940	51.5	2.1	0.2
n-decane	325.1	0.8320	52.0	2.1	0.2
	A = PEO,	B = PPO,	S = Benzene		
water	30.0	0.2	33.9	0.25	0.0015

pendence of the interfacial tension on bulk solution composition is not always obeyed in the case of free solutions of polymers or of low molecular weight components. The origin of the deviation from linearity lies in the preferential adsorption or depletion of one of the components at the interface, which causes the surface composition to differ from the bulk composition.[15] In the case of polymer solutions, when deviation from linearity is observed, it is found to occur at very low polymer concentrations. At larger concentrations of the polymer, the interfacial tension displays a linear dependence on solution composition.[15] The micellar interface considered in this work is somewhat different from the interface of a free polymer solution. Specifically, because of the localization of the A–B link at the interface, the segments of the A block are forced to be at the interface independent of any selective adsorption or depletion. Further, in a micellar aggregate saturated with the solubilizate, the volume fraction of polymer A within the core region is typically quite large so as to make the core a semidilute or concentrated solution. We anticipate that the difference between the surface and overall compositions in the micelle is smaller when compared to that in a free polymer solution. Consequently, the composition averaging of interfacial tension as expressed by eq 24 is assumed for our calculations. A more rigorous treatment of this problem on a fundamental basis remains for future work.

The interfacial tension σ_{AS} between polymer A and solvent S has been estimated[16] by the expression

$$\sigma_{AS} = (kT/l^2)(\chi_{AS}/6)^{1/2} \quad (25)$$

The above expression was derived for the interfacial tensions between two incompatible but symmetric homopolymers. In the present case of polymer–low molecular weight solvent interfacial tensions, eq 25 is expected to overestimate the interfacial tension somewhat, since it does not account for any mixing contributions at the interface due to the presence of the small molecular weight liquid. Estimates of this mixing contribution have been found to be relatively small compared to the value of σ_{AS} estimated from eq 25 as long as the A block and solvent S remained highly incompatible,[17] as in the present case. As a general rule, wherever possible, we recommend the use of experimentally measured values for σ_{AS} in the calculations of micellization and solubilization behavior.

Estimation of Model Parameters. To perform quantitative calculations, the values of parameters appearing in eq 17–25 are needed. In this paper, illustrative calculations have been carried out for poly(ethylene oxide)–poly(propylene oxide) block copolymer with water as the solvent and hydrocarbons as the solubilizates and also for the same block copolymer with benzene as the solvent and water as the solubilizate. Values for the molecular volumes of the solubilizates, the interaction parameters between the core block A and the solubilizates J, the interaction parameters between the solvent S and the A and B blocks of the copolymer, and the interfacial tensions between the solvent and the solubilizates are all summarized in Table I. Values for the Flory–Huggins interaction parameters have been estimated[4] by utilizing the Hildebrand–Scatchard solubility parameters approach. For calculating the values of m_A and m_B, the molecular volumes of the repeating units are taken to be 96.5 Å^3 for propylene oxide and 64.6 Å^3 for ethylene oxide. For all the systems, the numerical computations were carried out for m_A/m_B ranging from 0.1 to 10 and $m = m_A + m_B$ in the range 50–2500.

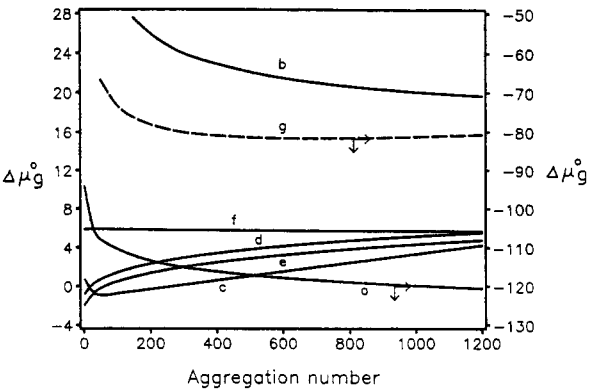

Figure 2. Free energy contributions as a function of the aggregation number g. The parameters D and η are not held constant but are assigned values that minimize the free energy per molecule of the micelle for each given aggregation number. The various contributions (a)–(f) are described in the text. The net free energy is given by curve g. Free energies are expressed in units of kT.

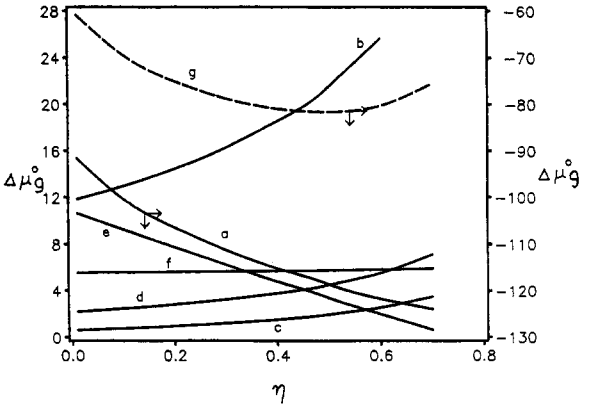

Figure 3. Free energy contributions as a function of the volume fraction η of the solubilizate in the micellar core. The parameters D and g are held constant and are assigned values that correspond to the global minimum of the free energy per molecule with respect to g, D, and η. The various contributions (a)–(f) are described in the text. The net free energy is given by curve g. Free energies are expressed in units of kT.

Results and Discussion

Physicochemical Interpretation of Solubilization Capacity. In our earlier paper,[9] the formation of finite spherical micelles in the absence of solubilizates has been interpreted in terms of the various free energy contributions (all defined per molecule of the copolymer) to micelle formation. An analogous interpretation can be provided in the presence of solubilizates from the free energy curves for solubilization shown in Figures 2 and 3. In Figure 2, the various free energy contributions are plotted against the aggregation number g. The remaining two independent variables D and η are not kept constant but are chosen

to be those values that minimize the free energy per molecule of the micelle for each given value of g. In Figure 3, the various free energy contributions are plotted as a function of the volume fraction of the solubilizate η. The remaining independent variables g and D are kept constant at the values corresponding to the global minimum of the free energy (i.e., with respect to g, D, and η) per molecule of the micelle. Thus Figure 2 helps illustrate how the equilibrium aggregation number is influenced by various free energy contributions, while Figure 3 reveals the importance of various contributions for the determination of the equilibrium uptake of the solubilizate.

The formation of micelles in preference to the singly dispersed state of the copolymer occurs because of the large negative free energy contribution arising from a change in the state of dilution of the solvent-incompatible A block following solubilization (curve a). In the absence of the solubilizates, this free energy contribution is a constant independent of the size of the micelle and hence does not govern the aggregation number of the micelle. However, in the presence of the solubilizate, this free energy also accounts for the swelling of the A blocks by the solubilizate J. This free energy decreases with an increase in the aggregation number g and is thus favorable to the growth of the aggregates. A second contribution favorable to the growth of the aggregates is provided by the interfacial energy (curve b). In general, the surface area per molecule of the micelle decreases with an increase in the aggregation number. Consequently, the positive interfacial free energy between the micellar core and the solvent decreases with increasing aggregation number of the micelle and thus this contribution promotes the growth of the micelle. The changes in the state of deformation of the A and the B blocks (curves c and d) and the change in the state of dilution of the B block (curve e) provide positive free energy contributions that increase with increasing aggregation number of the micelle. Therefore, these factors are responsible for limiting the growth of the micelle. More interestingly, when solvent S is a very good solvent for the B block, the positive free energy contributions resulting from changes in the states of dilution and of deformation of the B block outweigh the contribution resulting from the changes in the state of deformation of the A block. Under such conditions, the B block related free energy contributions strongly influence the structural properties of the equilibrium micelles. The free energy of localization (curve f) is found to be practically independent of g and thus has no influence over the determination of the equilibrium aggregation number. The net free energy of the micelle per molecule is shown by curve g. As one would expect, this free energy is negative and shows a minimum at the equilibrium aggregation number.

The free energy curves in Figure 3 show how the equilibrium extent of solubilization is determined for any given aggregation number. Curve a shows the large negative free energy contribution provided by the change in state of dilution of block A. This free energy decreases with an increase in the volume fraction of the solubilizate. This factor thus favors the uptake of the solubilizate within the micelle. One may note that the magnitude of this contribution is larger if the solubilizate–core block interaction parameter χ_{AJ} is lower and if the molecular size of the solubilizate m_J is smaller. Correspondingly, the capacity of the micelles for such solubilizates (i.e, the equilibrium value of η) will be larger. When micelles incorporate solubilizates, the radius of the micellar core and the interfacial area per molecule of the micellar core both increase. The former increases the positive free energy

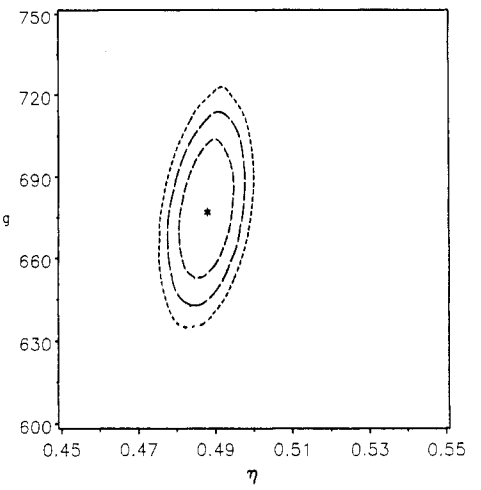

Figure 4. Distribution of the aggregation number and the solubilization capacity of the micelles at equilibrium. The solubilization capacity is expressed as the volume fraction of the solubilizate η within the core of micelles. The calculations are for benzene solubilized in PEO–PPO (molecular weight 12 500, 30% PPO) micelles present in water. The closed curves are the loci of sizes and compositions of aggregates present at identical concentrations. See the explanation in the text.

contribution arising from the increased deformation of the A block (curve c). The latter increases the positive free energy contribution associated with the micellar core–solvent interfacial free energy (curve b). Thus both these factors serve to restrict the swelling of the micellar core by the solubilizate and, consequently, the extent of solubilization. One may note that the increase in the positive interfacial free energy accompanying the uptake of solubilizates by the micelles (shown by curve b) is also dependent on the solubilizate–solvent interfacial tension σ_{SJ}. Therefore, given two solubilizates, the micellar capacity η will be larger for the solubilizate associated with a lower solubilizate–solvent interfacial tension σ_{SJ}. Further, the increase in the amount of solubilizate within a micelle of specified aggregation number also changes the state of deformation (curve d) as well as the state of dilution (curve e) of the B block in the shell region of the micelle. Of these two positive free energy contributions, the former increases with η, thus disfavoring solubilization, while the latter decreases with increasing η, thus favoring increased solubilization. The free energy of localization (curve f) is practically independent of η and thus has little influence over the nature and extent of solubilization. The net free energy of the micelle per molecule is represented by curve g. The minimum in this net free energy occurs at the equilibrium value for η. All the results described in the following sections can be interpreted in terms of the above-described free energy variations accompanying solubilization.

Validity of the Pseudophase Approximation. As mentioned earlier, the visualization of micelles as a pseudophase is quite satisfactory and very convenient when the aggregates are narrowly dispersed in size. Here, the size and composition distributions (namely, the dispersion in the values of variables g and j around their most probable values) have been calculated for a number of micellar systems containing the solubilizates. A typical result is shown in Figure 4 for benzene solubilized within PEO–PPO micelles in aqueous solutions. The volume fraction of the solubilizate within the micellar core η has been chosen as the independent variable in place of j in constructing this figure. The point enclosed by the closed curves corresponds to the most populous micelles, that is,

those aggregates whose concentration in the solution is the largest. The three closed curves surrounding this point are the loci of micellar sizes and compositions, corresponding to which the micellar concentrations are respectively 1, 2, and 3 orders of magnitude smaller compared to the concentration of the most populous micelles. One can observe that the aggregate concentrations fall off very rapidly when the values of g and η deviate from those of the most populous micelles represented by the point in Figure 4. Similar numerical calculations of the aggregate distributions for all the systems considered in this work indicate that the micelles are virtually monodispersed both in relation to the number of constituent block copolymer molecules as well as the number of solubilizate molecules. Therefore, it is quite satisfactory to simplify the calculations by invoking the pseudophase approximation and then estimating the micellar characteristics by the minimization of the free energy of an isolated micelle. The equilibrium micelle is obtained from the minimization of the free energy per molecule of the micelle with respect to the three independent variables R, D, and η.

$$\left.\frac{\partial}{\partial R}\left(\frac{\Delta\mu^{\circ}_{g}}{kT}\right)\right|_{D,\eta=\text{constant}} = 0$$
$$\left.\frac{\partial}{\partial D}\left(\frac{\Delta\mu^{\circ}_{g}}{kT}\right)\right|_{R,\eta=\text{constant}} = 0 \qquad (26)$$
$$\left.\frac{\partial}{\partial \eta}\left(\frac{\Delta\mu^{\circ}_{g}}{kT}\right)\right|_{D,R=\text{constant}} = 0$$

While performing the above minimization, for the purposes of simplifying the results, we expand the first logarithmic term in eq 21, retaining up to second-order terms. This is satisfactory because the volume fraction of the B blocks in the micellar shell region is expected to be small.

The following implicit equations for R, D, and η are obtained from eq 13 and 26 in conjunction with the geometrical relations eq 10–12. Equating the derivative with respect to R to zero, one obtains

$$R^3 = \left[\left[3m_A{}^2\left[\left(\frac{\sigma_{AS}l^2}{kT}\right) + \frac{\eta}{1-\eta}\left(\frac{\sigma_{SJ}l^2}{kT}\right)\right] + m_A{}^{3/2} + m_A m_B{}^{1/2}(R/D)\right] \Big/ \left[1 + \frac{m_A l^2}{R^2} + \left(\frac{m_A}{m_B}\right)\left(\frac{D}{R}\right)^2\right]\right] l^3 \qquad (27)$$

The free energy contributions from which the various terms in the above equation originate can be identified. In the numerator of eq 27, the first term arises from the interfacial free energy, the second term from A block deformation, and the third term from the B block dilution. In the denominator, the first term arises from the A block deformation, the second term from localization, and the last term from B block dilution. Similarly, when the derivative of the free energy with respect to D is equated to zero, one obtains

$$\frac{R^2(D/R)}{m_B l^2} - \frac{m_B{}^{1/2} l}{R(D/R)^2} + \frac{3}{(1+D/R)} + \frac{3m_B{}^2}{m_A} \times \frac{(1-\eta)(1+D/R)^2}{[(1+D/R)^3-1]^2}\left(\chi_{BS} - \frac{1}{2} - \frac{m_B}{m_A}\frac{(1-\eta)}{[(1+D/R)^3-1]}\right) = 0 \qquad (28)$$

Here, the first two terms originate from the B block deformation, the third term from localization, and the last term from the B block dilution. Finally, by equating the derivative of the free energy with respect to η to zero, one gets

$$\frac{3m_A l}{R(1-\eta)^2}\left(\frac{\sigma_{SJ}l^2}{kT}\right) + \frac{m_A}{m_J}\left(\frac{1}{1-\eta} + \frac{\ln\eta}{(1-\eta)^2} + \chi_{AJ}\right) + \frac{m_B{}^2}{m_A}\frac{1}{[(1+D/R)^3-1]}\left(\chi_{BS} - \frac{1}{2} - \frac{m_B}{m_A}\frac{(1-\eta)}{[(1+D/R)^3-1]}\right) = 0 \qquad (29)$$

In the above relation, the first term arises from the interfacial free energy, the second term is due to the A block dilution, and the last term arises from the B block dilution. One can thus clearly see which of the free energy contributions are relevant for the determination of each structural feature of the micelle, keeping the remaining parameters constant. Approximate analytical relations for R, D, and η can be obtained from eq 27–29 by retaining only the dominant terms in the equations. However, in this paper, detailed numerical computations have been carried out so as to improve the precision of the results.

The simultaneous numerical solution of the nonlinear algebraic equations (27)–(29) provides the values for the core radius R, the shell thickness D, and the solubilization capacity expressed as the volume fraction η of the micellar core, all corresponding to the equilibrium micelle. The critical micelle concentration expressed as a volume fraction of the copolymer in the solution is then calculated from eq 9, where the free energy of micellization is evaluated corresponding to the equilibrium micelle. In the present study, the nonlinear algebraic equations have been solved simultaneously by using the standard IMSL (International Mathematical and Statistical Library) subroutine called ZSCNT.

Table II
Solubilization of Hydrocarbons by PEO–PPO Micelles in Water (PEO(70%)–PPO(30%), Copolymer Molecular Weight = 12 500)

J	R, Å	D/R	η^a	$-\ln(\phi_1)_{cmc}$	g	D, Å
benzene	125	1.84	0.49 (0.51)	82.7	677	231
o-xylene	113	2.03	0.39 (0.33)	74.9	599	230
ethylbenzene	111	2.08	0.36 (0.41)	73.6	588	231
toluene	117	1.97	0.42 (0.40)	77.3	630	231
cyclohexane	105	2.21	0.27 (0.18)	71.7	578	233
n-hexane	88	2.54	0.10 (0.08)	66.4	415	224
n-heptane	87	2.56	0.08 (0.08)	65.9	405	223
n-octane	87	2.57	0.08 (0.08)	66.7	404	223
n-decane	85	2.61	0.06 (0.06)	65.0	386	221
none	80	2.72		64.0	342	217

[a] The numbers within the parentheses are experimental data.[4] Both experimental and theoretical values for η refer to the solubilization capacity of the micelles.

Comparison with Experimental Data. Experimental measurements of the solubilization capacities of aliphatic and aromatic hydrocarbons in poly(ethylene oxide)–poly(propylene oxide) (PEO–PPO) diblock copolymer micelles in water have been carried out in our earlier work[4] and these data are compared here against the predictions of the present theory. The polymer has a molecular weight of 12 500 and contains 30% by weight of the solvent-incompatible poly(propylene oxide) block. The molecular properties of the solubilizates and their interactions with PPO are listed in Table I. The predictions of the present theory are summarized in Table II. Also shown within the paranthesis are the experimentally measured values for the solubilization capacities. In general, the agreement

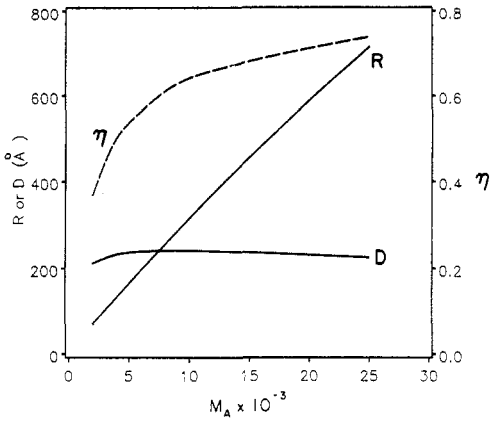

Figure 5. Core radius, shell thickness, and volume fraction of solubilizate benzene (at saturation) within the core of PEO–PPO micelles in water. The molecular weight of PEO is constant at 8750, while the molecular weight of PPO is varied as shown.

Table III
Influence of Copolymer Characteristics on the Solubilization of Benzene in Aqueous Solutions of PEO–PPO Micelles

M	M_A	m_A	m_B	R	D/R	η	g	$-\ln(\phi_1)_{cmc}$
4750	0.79	208	49	163	0.24	0.50	1453	94.2
6250	0.60	208	123	152	0.58	0.51	1154	90.4
8250	0.45	208	221	140	1.01	0.50	921	87.0
12500	0.30	208	429	125	1.84	0.49	677	82.7
15750	0.24	208	589	118	2.42	0.48	582	80.7
10750	0.19	111	429	70	3.00	0.37	279	46.4
14250	0.39	306	429	179	1.33	0.55	1187	116.7
17250	0.49	472	429	271	0.89	0.62	2244	171.8
20750	0.58	667	429	373	0.64	0.66	3665	232.5
33750	0.74	1389	429	716	0.32	0.74	9725	440.3

beween the experimental and measured values of η are reasonably satisfactory for all the solubilizates. Whereas the theory permits the prediction of all the structural features of the micelles, experimental data on these features are currently not available and hence the corresponding comparisons have not been possible.

The predicted results show a number of interesting features. The solubilization capacity for the solubilizates is larger if the core block is very compatible with the solubilizates, if the solubilizate–solvent interfacial tension is lower, and if the molecular volume of the solubilizate is smaller. Consequently, the aromatic molecules are found to display a larger solubilization limit compared to the aliphatic molecules in the block copolymer system considered here. The solubilization process is found to substantially increase the micellar core radius and decrease the critical micelle concentration. The larger the solubilization capacity, the more significant are the changes in R and the cmc. The increase in the core radius R results not only from the incorporation of the solubilizate but also because of the increasing number of block copolymer molecules that are accommodated within a micelle. This increase in the aggregation number g is more dramatic for a solubilizate whose uptake by the micelles is large. The dimensionless shell thickness D/R is found to decrease with increasing solubilization capacity of the micelles, while the shell thickness D is not very much affected by solubilization.

Generalized Scaling Relations. The dependence of the solubilization capacity and the other structural features of the micelles on the block copolymer size and composition have been examined through illustrative calculations for benzene as the solubilizate in PEO–PPO micelles present in aqueous solutions. Table III and Figures 5–8 summarize the calculated results. Figure 5 shows the

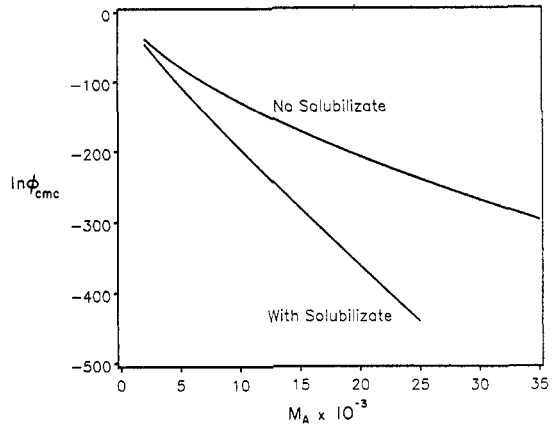

Figure 6. Cmc of micelles containing solubilizates as well as solubilizate-free micelles. The system is identical with that described in Figure 5.

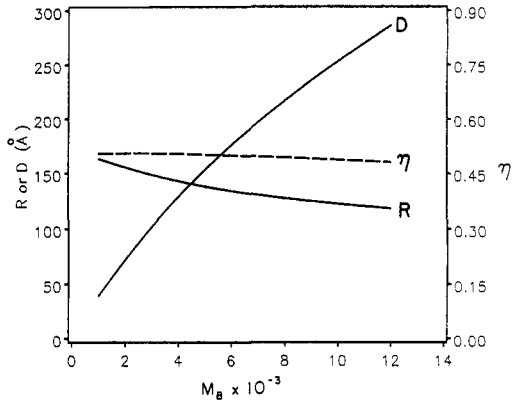

Figure 7. Core radius, shell thickness, and volume fraction of solubilizate benzene (at saturation) within the core of PEO–PPO micelles in water. The molecular weight of PPO is constant at 3750, while the molecular weight of PEO is varied as shown.

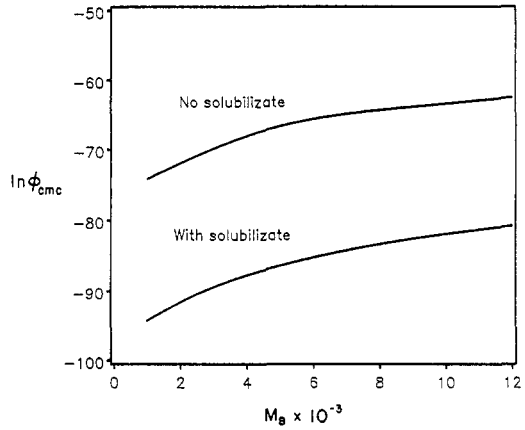

Figure 8. Cmc of micelles containing solubilizates as well as solubilizate-free micelles. The system is identical with that described in Figure 7.

dependence of R, D, and η on the molecular weight of the poly(propylene oxide) block, keeping the molecular weight of the poly(ethylene oxide) block constant at 8750. It is found that the core radius R and the solubilization capacity η change significantly, whereas the shell thickness D remains more or less unaffected. The corresponding variation in the cmc is plotted in Figure 6. The cmc is lower compared to that of the solubilizate-free solutions and the deviation caused by the presence of the solubilizate increases with increasing size of the core block PPO. It is possible to interpret these variations, recognizing that the core block is considered to constitute the site of solubili-

zation. Therefore, a change in the size of the core block directly influences the values of R, η, and the cmc. Since the shell thickness is primarily dependent on the solvent-compatible B block (PEO), the value of D is only very weakly dependent on m_A. Figures 7 and 8 present similar calculated results, but as a function of the size of the shell block PEO, keeping the molecular weight of the core block PPO constant at 3750. The calculations show that the variation in the magnitude of m_B affects the core radius R and η in addition to having a more significant influence on the shell thickness D. An increase in the value of m_B causes a reduction in both R and η. In solubilizate-free systems, the shell block B influences the micellar radius R (or equivalently, the aggregation number g) significantly, especially if the solvent S is a good solvent for the B block, as is the case for PEO–water.[9] The present calculations show that in the presence of the solubilizates, the magnitude of the influence of the B blocks is somewhat reduced, while being qualitatively similar to that in solubilizate-free systems. The larger the solubilization capacity of the micelles, the less prominent is the role played by the B block–solvent S interactions. The variation in the cmc due to a change in the molecular weight of PEO (Figure 8) parallels the behavior observed in the absence of the solubilizate. The difference between the two curves is a measure of the influence of the solubilizate on the cmc and this difference is practically uninfluenced by the magnitude of m_B.

By correlating the calculated numerical results (Figures 5–8 and Table III), scaling relations between micellar size characteristics and the block sizes m_A and m_B have been obtained. For the PEO–PPO micelles in water, with benzene as the solubilizate, it is found that

$$R \propto m_A^{0.92} m_B^{-0.13}, \qquad g \propto m_A^{1.42} m_B^{-0.39}, \qquad D \propto m_A^{-0.08\sim-0.125} m_B^{0.79}, \qquad \eta \propto m_A^{0.17} m_B^{-0.017} \tag{30}$$

One may compare these scaling relations against those obtained[9] in the absence of the solubilizate. For the PEO–PPO–water system, it was found that

$$R \propto m_A^{0.73} m_B^{-0.17}, \qquad g \propto m_A^{1.19} m_B^{-0.51}, \qquad D \propto m_A^{0.06} m_B^{0.74} \tag{31}$$

By comparison of eq 30 and 31, it can be seen that the scaling relations are modified in the presence of the solubilizate. The solvent-compatible B block continues to influence the magnitude of the micellar core parameters R and g, but the influence is somewhat diminished by the presence of the solubilizate.

One may note that the scaling relations (30) and (31) are specific in the sense that they depend on the nature of the solubilizate as well as on the block copolymer–solvent system. To allow easy comparison between experimental data and the present theory, we have also developed general predictive relations between the solubilization characteristics and the molecular properties of the block copolymer–solvent–solubilizate systems. These predictive relations were developed on the basis of the numerical results obtained for the solubilization of various hydrocarbons in PEO–PPO micelles present in water and for the solubilization of water in PEO–PPO micelles present in benzene. Since a range of molecular parameters are encompassed by these systems, it is expected that the general relations developed based on them would have a reasonably wide range of applicability. It must, however, be noted that these equations are valid for micelles having spherical structure only. Analogous equations for systems exhibiting nonspherical aggregate structures will be presented in a later paper. The correlation of the various numerical results yields the following relation

$$R = \left[\left[3m_A^2\left[\left(\frac{\sigma_{AS}l^2}{kT}\right) + \frac{\eta}{1-\eta}\left(\frac{\sigma_{SJ}l^2}{kT}\right)\right] + m_A^{3/2} + m_A m_B^{1/2}(R/D)\right]^{1/3} \Big/ [1 + m_A^{-1/3} + (m_A/m_B)(D/R)^2]^{1/3}\right] l \tag{32}$$

Given eq 32 for the radius of the micellar core and the geometrical relation for a sphere (eq 10 and 12), the aggregation number g of the equilibrium micelle can be calculated from

$$g = \left[\left[4\pi m_A\left[\left(\frac{\sigma_{AS}l^2}{kT}\right) + \frac{\eta}{1-\eta}\left(\frac{\sigma_{SJ}l^2}{kT}\right)\right] + \frac{4\pi}{3}m_A^{1/2} + \frac{4\pi}{3}m_B^{1/2}(R/D)\right] \Big/ [1 + m_A^{-1/3} + (m_A/m_B)(D/R)^2]\right](1-\eta) \tag{33}$$

The dimensionless shell thickness can be calculated from

$$\frac{D}{R} = 0.867\left[\frac{1}{2} + \frac{m_A^2 m_B}{(m_A + m_B)^3}(1-\eta) - \chi_{BS}\right]^{1/5} m_A^{-8/11} m_B^{6/7} (1-\eta)^{6/11} \tag{34}$$

The solubilization capacity of the block copolymer micelle at equilibrium can be obtained from

$$1 - \eta = 1.154\left(\frac{\sigma_{SJ}l^2}{kT}\right)^{3/5} (1 - \chi_{AJ})^{-1/20}\left(\frac{1}{2} + \frac{m_A^2 m_B}{(m_A + m_B)^3} - \chi_{BS}\right)^{-1/4} m_A^{-5/16} m_J^{7/15} \tag{35}$$

The correlation equations (32)–(35) have been generated retaining the structure of the equations suggested by the free energy minimization conditions, eq 27–29. Indeed, the correlation equation for R is practically identical with eq 27 but for a minor approximation in the relatively insignificant second term in the denominator (whose origin has been identified earlier to be the localization free energy). Equation 33 follows from eq 32 and the exact geometrical relations defining the micellar structure. Equations 34 and 35 are similarly built by retaining the dominant terms in eq 28 and 29, respectively. The numerical coefficients and the various exponents are then slightly adjusted in order to improve the fit between the numerical results and the correlating equations. For the range of parameters investigated in this paper, the above correlation equations describe the detailed numerical predictions within 1% root mean square (rms) deviation for R and g, 8% for D/R, and 2% for η.

The predictions of the theory can thus be obtained conveniently from the above scaling relations as follows. Given any block copolymer–solvent–solubilizate system, knowing the relevant molecular parameters, one can explicitly compute the solubilization capacity of the micelles expressed as η from eq 35. By introduction of this value into eq 34, the dimensionless shell thickness (D/R) can be

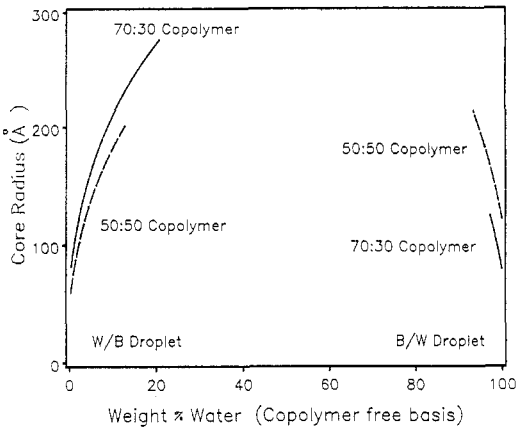

Figure 9. Core radius of equilibrium micelles of PEO–PPO containing solubilizate at various compositions of the solvent–solubilizate system. The region in the left describes micelles present in benzene and containing water as the solubilizate. The region on the right describes micelles present in water and containing benzene as the solubilizate. The molecular weight of the copolymer is 12 500, and the two copolymer samples contain 30 and 50 wt % PPO.

determined. Introducing the values for (D/R) and η in eq 32 and 33 allows one to directly estimate the core radius R and the aggregation number g of the micelle, respectively. The scaling relations presented in the treatment of micellization[9] are recovered, if the solubilizate volume fraction η is made equal to zero in eq 32–34. Further, eq 32–34 can also be utilized to calculate the micellar structural parameters for any arbitrary value of η that is smaller than the saturation capacity predicted by eq 35.

Region of Existence of Spherical Micelles. Since spherical micellar structures have been assumed in the present theory, a natural question is whether such geometry is favored by equilibrium over the entire composition range (on a copolymer-free basis) of the solvent–solubilizate system. To answer this question, we have determined the domain of the existence of spherical micelles on the basis of the present theory for the PEO–PPO block copolymer–water–benzene system. A block copolymer molecular weight of 12 500 and two block compositions, namely 30 and 50% by weight of the poly(propylene oxide) block, have been chosen for the illustrative calculations. For a given extent of solubilization η (which can vary from 0 to the saturation value predicted by eq 35), the corresponding structural parameters R, D, and g of the equilibrium micelles have been computed by using eq 32–34. With the value of η and the amount of copolymer in the total system known, the relative amounts of the solvent, the solubilizate, and the copolymer have all been calculated. This allows the determination of the copolymer-free composition of the solvent–solubilizate system, corresponding to the equilibrium micelle. The results are shown in Figure 9 in the form of a plot of the core radius of the micelle against the copolymer-free composition of the system. A system containing 10 wt % of the block copolymer is used in plotting Figure 9 for illustrative purposes. The two terminal points in each of the four lines correspond to solubilizate-free micelles and micelles saturated with the solubilizate. At all intermediate points in these lines, the uptake of the solubilizate by the micelles is below their solubilization capacity. One can see that the solubilization limits predicted by the spherical micellar model encompass only a part of the composition space in the diagram. Both in the benzene-rich and in the water-rich ends, the theory predicts the solubilization of water and benzene, respectively, in spherical micelles. The composition space between these ends must be characterized by nonspherical aggregate structures. This composition space becomes enlarged if the amount of block copolymer in the system is decreased. One may note that even in the region where the existence of spherical micelles is predicted here, it is possible that nonspherical aggregates may exist. This situation can be clarified only after an examination of the free energies of solubilization in nonspherical structures. This will be attempted for cylindrical and lamellar aggregate structures in a latter paper.

Conclusions

In this paper, a theory of solubilization of low molecular weight compounds in block copolymer micelles present in selective solvents is developed. A spherical micellar structure is assumed. All the solubilizate molecules are considered to be located within the core region of the micelles from where the solvent and the solvent-compatible block are completely excluded. The change in free energy accompanying solubilization is modeled by considering all the physicochemical changes that occur on solubilization. Specifically, the changes in the states of dilution and deformation of the two polymer blocks, the localization of the copolymer, and the formation of a micellar interface all contribute to the free energy of solubilization. The theory allows one to predict the critical micelle concentration, the size and composition distribution of the micelles, and various average properties such as the aggregation number, the solubilization capacity, and the radius and the shell thickness of the micelles. Illustrative calculations have been made for water-soluble PEO–PPO copolymer with hydrocarbon solubilizates and for benzene-soluble PEO–PPO copolymer with water as the solubilizate. The calculations show that micelles are practically monodispersed in their aggregation numbers as well as in the extent of solubilization. The solubilization capacity and the structural parameters of the micelles are significantly influenced by the interactions between the solubilizate and the core block of the copolymer and also by the solubilizate–solvent interfacial tension. The solubilization behavior and the dimensions of the micelles are also affected by the interactions between the solvent and the solvent-compatible shell block of the copolymer. However, the influence of these interactions is somewhat diminished when compared to the behavior of the corresponding solubilizate-free systems. Scaling relations have been developed relating the micellar core radius, the shell thickness, the aggregation number, and the volume fraction of the solubilizate within the core to the properties of the copolymer, the solvent, and the solubilizate. These relations permit explicit calculations of all the important results predicted by the present theory. Finally, the domain of existence of spherical micelles is shown to extend over only a small region of the allowed composition space of the system. The extension of the present theory to nonspherical micellar structures will be discussed in a latter paper.

Appendix

Free Energy of Deformation of Nonuniformly Stretched Chains. In developing the free energy expressions for the change in state of dilution and deformation of the A and the B blocks (eq 17, 18, 21, and 22), we have treated the core and the shell regions to be uniform in concentrations and the elastic deformation of the chains to be uniform along the chain length. Consequently, the free energy expressions developed by Flory[13] for the uniform deformation of the chains have been used in our calculations. This is entirely satisfactory if the system

dimensions are very large so as to make the consideration of the system boundaries irrelevant. However, in small systems such as micelles, because of the aggregate geometry, the maintenance of uniform concentrations in the core and the shell regions is strictly not possible while simultaneously allowing for uniform deformation of the chains. For example, in spherical micelles containing solubilizates, the incremental volume available for the polymer segments in both core and shell regions increases with increasing radial distance from the center of the micelle. Consequently, the chains should deform nonuniformly along the radius of the micelle in order to ensure the constancy of density or concentrations. We summarize below the expressions for the elastic deformation free energies of the A and the B blocks within the micelle, taking into account the nonuniform stretching of the chains. We also rederive the main results of this paper for this nonuniform chain deformation model.

As part of his treatment of microdomains in block copolymer melts, Semenov[18] developed analytical expressions for the elastic deformation free energies of the A and the B blocks, taking into account the nonuniformity in the stretching of the chains. Here, the nonuniformity in chain stretching is necessitated by the requirement that chain densities inside the core and the matrix regions of the domain structure must remain constant. In this treatment, a distribution of the free ends of the chains is also taken into consideration, namely, that the free ends of all A chains need not be at $r = 0$ and the free ends of all B chains need not be at $r = R + D$. Semenov obtained the following results (in our notations) for the elastic deformation free energies of A and B blocks:

$$(\mu^\circ_g)_{\text{def,A}} = \frac{3\pi^2}{80}\frac{R^2}{m_A l_A^2} \tag{A-1}$$

$$(\mu^\circ_g)_{\text{def,B}} = \frac{1}{2}\frac{R^2 l_B}{m_A l_A^3}\left[1 - \frac{R}{R+D}\right] \tag{A-2}$$

The above results have been adapted by Zhulina and Birshtein[19] to the situation where the core and the matrix regions of the domain structure of a block copolymer are both swollen by a solvent. In this case, the assumption of uniform concentrations in the core and the matrix regions necessitates the nonuniform stretching of the chains. Zhulina and Birshtein used the "blob" concept of de Gennes,[12] namely, that the swollen A and B block regions can be effectively represented as consisting of n_A and n_B blobs of characteristic sizes ζ_A and ζ_B, the volume fractions of polymer inside the blobs being ϕ_A and ϕ_B, respectively, to modify the expressions for the deformation free energies by Semenov.[18] Thus

$$(\mu^\circ_g)_{\text{def,A}} = \frac{3\pi^2}{80}\frac{R^2}{n_A \zeta_A^2} \tag{A-3}$$

$$(\mu^\circ_g)_{\text{def,B}} = \frac{1}{2}\frac{R^2 \zeta_B}{n_A \zeta_A^3}\left[1 - \frac{R}{R+D}\right] \tag{A-4}$$

This approach is directly applicable to the present discussion of solubilization, since we consider the core and the shell regions to be uniform in concentrations.

One can write eq A-3 and A-4 explicitly in terms of known molecular parameters. The number of blobs n_i (here i can refer to A or B) and their size ζ_i are related[12] to the number of segments m_i and the segment length l_i through the concentration variable ϕ_i. When the solvent S is a good solvent for the B blocks and the solubilizate J is a good solvent for the A blocks, one can write

$$n_i = m_i \phi_i^{5/4}\left(\frac{1}{2} - \chi_i\right)^{3/4} \tag{A-5}$$

$$\zeta_i = l_i \phi_i^{-3/4}\left(\frac{1}{2} - \chi_i\right)^{-1/4} \tag{A-6}$$

When i = A, $\chi_i = \chi_{AJ}$, and when i = B, $\chi_i = \chi_{BS}$. Given the geometrical relations characterizing the micelle (eq 10–12), the volume fractions ϕ_A and ϕ_B can be expressed as

$$\phi_A = 1 - \eta, \qquad \phi_B = \frac{m_B}{m_A}\frac{(1-\eta)}{[(1 + D/R)^3 - 1]} \tag{A-7}$$

Expression A-3 for the core block A deformation free energy thus gets rearranged to

$$(\mu^\circ_g)_{\text{def,A}} = \frac{3\pi^2}{80}\frac{R^2}{m_A l^2}\left(\frac{1-\eta}{1/2 - \chi_{AJ}}\right)^{1/4} \tag{A-8}$$

For the range of molecular parameters considered in this paper, the above equation reduces approximately to

$$(\mu^\circ_g)_{\text{def,A}} = (0.3 \sim 0.4)\frac{R^2}{m_A l^2} \tag{A-9}$$

This estimate is to be compared against eq 18 on the basis of the uniform stretching model, namely

$$(\mu^\circ_g)_{\text{def,A}} = \frac{1}{2}\left[\frac{R^2}{m_A l^2} + \frac{2m_A^{1/2} l}{R} - 3\right] \tag{A-10}$$

For all practical purposes, there is very little difference between the estimates of the elastic deformation free energy calculated assuming nonuniform chain deformation and that calculated on the basis of uniform chain deformation, for the core block A.

For the shell block B, expression A-4 can be rearranged as

$$(\mu^\circ_g)_{\text{def,B}} = \frac{1}{2}\frac{R^2}{m_B l^2}[(1 + D/R)^3 - 1]\left(\frac{D/R}{1 + D/R}\right) \times \left[\left(\frac{1-\eta}{1/2 - \chi_{BS}}\right)\frac{m_B}{m_A}\frac{1}{[(1 + D/R)^3 - 1]}\right]^{1/4} \tag{A-11}$$

With the approximation $[(1 + D/R)^3 - 1] = (1 + D/R)^3$, eq (A-11) simplifies to

$$(\mu^\circ_g)_{\text{def,B}} = \frac{1}{2}\frac{D^2}{m_B l^2}\left[\left(1 + \frac{R}{D}\right) \times \left(\frac{1-\eta}{1/2 - \chi_{BS}}\right)^{1/4}\left(\frac{m_B}{m_A}\right)^{1/4}\left(1 + \frac{D}{R}\right)^{1/4}\right] \tag{A-12}$$

For the range of molecular parameters considered in this paper, the quantity within the square brackets is approximately between 2 and 4. This estimate of the deformation free energy is to be compared against eq 22 on the basis of the uniform chain stretching description, namely

$$(\mu^\circ_g)_{\text{def,B}} = \frac{1}{2}\left[\frac{D^2}{m_B l^2} + \frac{2m_B^{1/2} l}{D} - 3\right] \tag{A-13}$$

It can be seen that the uniform chain stretching model appreciably underestimates the elastic deformation energy when compared to the nonuniform chain stretching model for the shell block B.

The functional forms of the deformation free energies based on uniform and nonuniform chain stretching models are essentially similar to one another. If the equations

based on nonuniform stretching (eq A-8 and A-11) are used in place of the equations based on the uniform stretching (eq A-10 and A-13), one can expect some changes in the numerical results. Obviously, all the qualitative features of the solubilization model remain the same. Because the new expressions for the deformation free energies are weak function of η, one may expect insignificant changes in the predictions for the volume fraction η of the solubilizate. As the B block deformation free energies are now appreciably larger, one may anticipate that equilibrium will favor somewhat smaller values for D than those predicted in the paper. The core radius R and the aggregation number g will be correspondingly decreased somewhat.

Replacing eq A-10 and A-13 with eq A-8 and A-11 in the free energy of solubilization (thus accounting for nonuniform chain deformation), we obtain the following relations corresponding to the minimum of the free energy in place of eq 27–29:

$$R^3 = \left[3m_A^2 \left[\left(\frac{\sigma_{AS} l^2}{kT} \right) + \frac{\eta}{1-\eta} \left(\frac{\sigma_{SJ} l^2}{kT} \right) \right] \Big/ \left[\frac{3}{4} \left(\frac{1-\eta}{1/2 - \chi_{AJ}} \right)^{1/4} + \frac{m_A l^2}{R^2} + \left(\frac{1-\eta}{1/2 - \chi_{BS}} \right)^{1/4} \left(\frac{m_A}{m_B} \right)^{3/4} \left(\frac{D}{R} \right) \left(1 + \frac{D}{R} \right)^{5/4} \right] \right] l^3 \quad (27')$$

$$\left[\frac{1}{2} \frac{R^2}{m_B l^2} \left(\frac{m_B}{m_A} \right)^{1/4} \left(\frac{1-\eta}{1/2 - \chi_{BS}} \right)^{1/4} \left(1 + \frac{D}{R} \right)^{1/4} \left(1 + \frac{9}{4} \frac{D}{R} \right) \right] + \frac{3}{(1 + D/R)} + \frac{3m_B^2}{m_A} \frac{(1-\eta)(1 + D/R)^2}{[(1 + D/R)^3 - 1]^2} \times \left(\chi_{BS} - \frac{1}{2} - \frac{m_B}{m_A} \frac{(1-\eta)}{[(1 + D/R)^3 - 1]} \right) = 0 \quad (28')$$

$$\frac{3m_A l}{R(1-\eta)^2} \left(\frac{\sigma_{SJ} l^2}{kT} \right) + \frac{m_A}{m_J} \left(\frac{1}{1-\eta} + \frac{\ln \eta}{(1-\eta)^2} + \chi_{AJ} \right) - \left[\left(\frac{3\pi^2}{320} \right) \frac{R^2}{m_A l^2} \left(\frac{1}{1/2 - \chi_{AJ}} \right)^{1/4} \right] \left(\frac{1}{1-\eta} \right)^{3/4} + \frac{m_B^2}{m_A} \frac{1}{[(1 + D/R)^3 - 1]} \left(\chi_{BS} - \frac{1}{2} - \frac{m_B}{m_A} \frac{(1-\eta)}{[(1 + D/R)^3 - 1]} \right) \left(\frac{1 + 3(D/R)}{1 + (9/4)(D/R)} \right) = 0 \quad (29')$$

From the above free energy minimum conditions, the equilibrium properties of micelles containing solubilizates can be obtained. As before, from eq 27′ we can write an expression for the core radius R by making a minor approximation in the term arising from the localization free energy. Thus we obtain

$$R = \left[\left[3m_A^2 \left[\left(\frac{\sigma_{AS} l^2}{kT} \right) + \frac{\eta}{1-\eta} \left(\frac{\sigma_{SJ} l^2}{kT} \right) \right] \right]^{1/3} \Big/ \left[\frac{3}{4} \left(\frac{1-\eta}{1/2 - \chi_{AJ}} \right)^{1/4} + m_A^{-1/3} + \left(\frac{1-\eta}{1/2 - \chi_{BS}} \right)^{1/4} \left(\frac{m_A}{m_B} \right)^{3/4} \left(\frac{D}{R} \right) \left(1 + \frac{D}{R} \right)^{5/4} \right]^{1/3} \right] l \quad (32')$$

Given the geometrical properties of the micelle (eq 10–12), one can compute the aggregation number g from the core radius R as follows:

$$g = 4\pi m_A (1-\eta) \times \left[\left(\frac{\sigma_{AS} l^2}{kT} \right) + \frac{\eta}{1-\eta} \left(\frac{\sigma_{SJ} l^2}{kT} \right) \right] \Big/ \left[\frac{3}{4} \left(\frac{1-\eta}{1/2 - \chi_{AJ}} \right)^{1/4} + m_A^{-1/3} + \left(\frac{1-\eta}{1/2 - \chi_{BS}} \right)^{1/4} \left(\frac{m_A}{m_B} \right)^{3/4} \left(\frac{D}{R} \right) \left(1 + \frac{D}{R} \right)^{5/4} \right] \quad (33')$$

The dimensionless shell thickness D/R can be computed from the solution of eq 28′. Since the form of eq 28′ is essentially similar to the form of eq 28, the structure of the correlation equation can remain identical for eq 34 and the following eq 34′, the only change being in the exponent of one of the factors. We obtain

$$\frac{D}{R} = 0.867 \left[\frac{1}{2} + \frac{m_A^2 m_B}{(m_A + m_B)^3} (1-\eta) - \chi_{BS} \right]^{1/5} m_A^{-8/11} m_B^{6/7} (1-\eta)^{9/11} \quad (34')$$

As mentioned earlier, since the η dependence contained within the deformation free energies is small, the expression for η takes on a form identical with eq 35 with the exceptions that the leading coefficient and the exponent on the factor containing χ_{BS} are different:

$$1 - \eta = 0.802 \left(\frac{\sigma_{SJ} l^2}{kT} \right)^{3/5} (1 - \chi_{AJ})^{-1/20} \left(\frac{1}{2} + \frac{m_A^2 m_B}{(m_A + m_B)^3} - \chi_{BS} \right)^{-4/7} m_A^{-5/16} m_J^{7/15} \quad (35')$$

The fit of the correlation equations (32′)–(35′) to the numerical results retains the same order of accuracy as the fit of eq 32–35 to their corresponding numerical results. Specifically, the percent root mean square deviations are less than 1 for R and g, less than 9 for D/R, and less than 6 for η. The expressions for R, g, and D/R presented above can be used to calculate the structural features of the micelles in the absence of solubilizates if the chain deformation is modeled on the basis of nonuniform chain stretching. Analogous scaling relations assuming uniform deformation of the polymer chains can be obtained from ref 9.

In summary, one can observe that for a given value of D/R, eq 32′ will predict a somewhat smaller value for R compared to eq 32. Correspondingly, eq 33′ will predict a somewhat smaller value for the aggregation number g when compared to eq 33. The value of D/R for given block size and interaction parameters is somewhat smaller if eq 34′ is used when compared to eq 34. The volume fraction of the solubilizate is only weakly affected when the modified expressions for the deformation free energies are used. Typically, the values for D and R predicted by the free energy expressions that account for nonuniform chain stretching are smaller by up to 10% compared to the predictions based on the uniform stretching model.

Nomenclature

D	thickness of the micellar shell
g	aggregation number of the micelle
g_n	number-average aggregation number of the micelles
g_w	weight-average aggregation number of the micelles
g_z	z-average aggregation number of the micelles
k	Boltzmann constant

l effective length of the segment
m_A effective number of repeating units in block A of the copolymer
m_B effective number of repeating units in block B of the copolymer
m_J molecular volume ratio between the solubilizate J and the solvent S
M molecular weight of the block copolymer
M_A molecular weight of the A block of the copolymer
M_B molecular weight of the B block of the copolymer
R radius of the core of the micelle
$R_{\infty A}$ radius of the swollen A block in the singly dispersed copolymer
$R_{\infty B}$ radius of the swollen B block in the singly dispersed copolymer
T temperature of the system
v_S molecular volume of the solvent S
v_J molecular volume of the solubilizate J
V_{SH} volume of the micellar shell region
V_C volume of the micellar core region
$v_{\infty A}$ volume of the swollen A block in the singly dispersed copolymer
$v_{\infty B}$ volume of the swollen B block in the singly dispersed copolymer
v_A molecular volume of the A block of the copolymer
v_B molecular volume of the B block of the copolymer
X_1 mole fraction of the singly dispersed copolymer molecules in solution
X_{1J} mole fraction of the singly dispersed solubilizate molecules in solution
X_{gj} mole fraction of micellar aggregates containing g copolymer and j solubilizate molecules
α_A chain expansion parameter for block A in singly dispersed copolymer
α_B chain expansion parameter for block B in singly dispersed copolymer
η volume fraction of the solubilizate within the micellar core
μ°_S standard chemical potential of the pure solvent phase
μ°_1 standard chemical potential of the singly dispersed copolymer in infinitely dilute solution
μ°_{1J} standard chemical potential of the singly dispersed solubilizate in infinitely dilute solution
μ^*_{1J} standard chemical potential of the pure solubilizate phase
μ°_{gj} standard chemical potential of the micelle (containing g copolymer and j solubilizate molecules) in an infinitely dilute solution
σ_{AS} interfacial tension between the micellar core block A and the solvent S
σ_{SJ} interfacial tension between the solubilzate J and the solvent S
ϕ_1 volume fraction of singly dispersed copolymer in the solution
ϕ_{1J} volume fraction of singly dispersed solubilizate in the solution
ϕ_{gj} volume fraction of micelles containing g copolymer and j solubilizate molecules in the solution
ϕ_p volume fraction of the polymer A in the monomolecular globule
ϕ_A volume fraction of the block A in the core region of the micelle
ϕ_B volume fraction of the block B in the shell region of the micelle
χ_{AS} Flory–Huggins interaction parameter between the A block and the solvent S
χ_{BS} Flory–Huggins interaction parameter between the B block and the solvent S
χ_{AJ} Flory–Huggins interaction parameter between the A block and the solubilizate J

Registry No. (PEO)(PPO) (block copolymer), 106392-12-5; benzene, 71-43-2; *o*-xylene, 95-47-6; ethylbenzene, 100-41-4; toluene, 108-88-3; cyclohexane, 110-82-7; *n*-hexane, 110-54-3; *n*-heptane, 142-82-5; *n*-octane, 111-65-9; *n*-decane, 124-18-5.

References and Notes

(1) Tuzar, Z.; Kratochvil, P. *Adv. Colloid Interface Sci.* **1976**, *6*, 201.
(2) Price, C. In *Development of Block Copolymers I*; Goodman, I., Ed.; Applied Science Publishers: London, 1982; p 39.
(3) Riess, G.; Bahadur, P.; Hurtrez, G. In *Encyclopedia of Polymer Science and Engineering*; Wiley: New York, 1985; p 324.
(4) Nagarajan, R.; Barry, M.; Ruckenstein, E. *Langmuir* **1986**, *1*, 337.
(5) de Gennes, P.-G. In *Solid State Physics*; Liebert, J., Ed.; Academic Press: New York, 1978; Suppl. 14, p 1.
(6) Liebler, L.; Orland, H.; Wheeler, J. C. *J. Chem. Phys.* **1983**, *79*, 3550.
(7) Noolandi, J.; Hong, M. H. *Macromolecules* **1983**, *16*, 1443.
(8) Whitmore, D.; Noolandi, J. *Macromolecules* **1985**, *18*, 657.
(9) Nagarajan, R.; Ganesh, K. *J. Chem. Phys.* **1989**, *90*, 5843.
(10) Nagarajan, R.; Ruckenstein, E. *Sep. Sci. Technol.* **1981**, *16*, 1429. Nagarajan, R.; Chaiko, M. A.; Ruckenstein, E. *J. Phys. Chem.* **1984**, *88*, 2916.
(11) Nagarajan, R. *Colloids Surf.*, submitted for publication.
(12) de Gennes, P.-G. *Scaling Concepts in Polymer Physics*; Cornell University Press: Ithaca, NY, 1979.
(13) Flory, P. J. *Principles of Polymer Chemistry*; Cornell University Press: Ithaca, NY, 1962.
(14) Stockmayer, W. H. *J. Polym. Sci.* **1955**, *15*, 595.
(15) Siow, K. S.; Patterson, D. *J. Phys. Chem.* **1973**, *77*, 356.
(16) Helfand, E.; Tagami, Y. *J. Polym. Sci. B* **1971**, *9*, 741. Helfand, E.; Sapse, A. M. *J. Chem. Phys.* **1975**, *62*, 1327.
(17) Munch, M. R.; Gast, A. P. *Macromolecules* **1988**, *21*, 1360.
(18) Semenov, A. N. *Sov. Phys. JETP* **1985**, *61*, 733.
(19) Zhulina, Ye. B.; Birshtein, T. M. *Polym. Sci. USSR* **1987**, *29*, 1678.